Appendix A: Turbulence properties

Sub-grid turbulent diffusion (K_S) and the turbulent kinetic energy dissipation rate (ε)

The Smagorinsky's turbulence closure term [1], for the sub-grid turbulent diffusion (K_S) is calculated according to [2]:

$$K_S = (f_D C_s \Delta)^2 \sqrt{\frac{1}{2}\left(-\frac{\partial u_z}{\partial x}+\frac{\partial u_x}{\partial z}\right)^2+\left(\frac{\partial u_x}{\partial x}\right)^2+\left(\frac{\partial u_z}{\partial z}\right)^2} \qquad \text{(Eq. A1)}$$

Here, C_s is the Smagorinsky constant set to 0.2, Δ the size of the spatial discretization and u_z and u_x are the velocities in the vertical and horizontal dimension, respectively. The near sea surface turbulence shares many characteristics of that of a wall [3,4]. f_D describes the wall effect of the sea-surface on advection and diffusion ('law of the wall'), which is given by the van Driest wall damping function [5]:

$$f_D = 1-\exp\left(-\frac{y^+}{A}\right)^2 \qquad \text{(Eq. A2)}$$

where A is the van Driest constant ($A = 26$) and y^+ the dimensionless distance from the sea surface according to $y^+ = \frac{u_\tau z}{\upsilon}$. Here υ is the kinematic viscosity (1.05e^{-6} m^2 s^{-1} for seawater of 35 PSU and 20°C) and $u_\tau = \sqrt{\tau_w / \rho}$ is the frictional velocity scale, with ρ being the density of sea water and τ_w the wall shear stress $\tau_w = \mu\sqrt{\left(\frac{\partial u_x}{dz}\right)^2}$, where μ is the dynamics viscosity set to 0.001 kg m^{-1} s^{-1} (for seawater of 35 PSU and 20°C).

In free convective system and within the mixed layer the turbulent kinetic energy dissipation rate ε (W kg^{-1}) is equal to is the surface buoyancy flux J_0^b and remains relatively similar over the entire depth [4]. In such systems the vertical velocity scales according to $u_z = (J_0^b h_z)^{1/3}$ [6,7]. By replacing J_0^b with ε and solving for ε we can describe energy dissipation according to [4,8]:

$$\varepsilon = \frac{u_z^3}{h_z} \qquad \text{(Eq. A3)}$$

Using the mixing length time scale τ, with $\tau = 12$ hours [7], modelled values of ε ranging from ~1.25*10^{-10} W kg-1 at $h_z = 100m$ to ~5*10^{-08} W kg^{-1} $h_z = 2000m$ (figure A1).

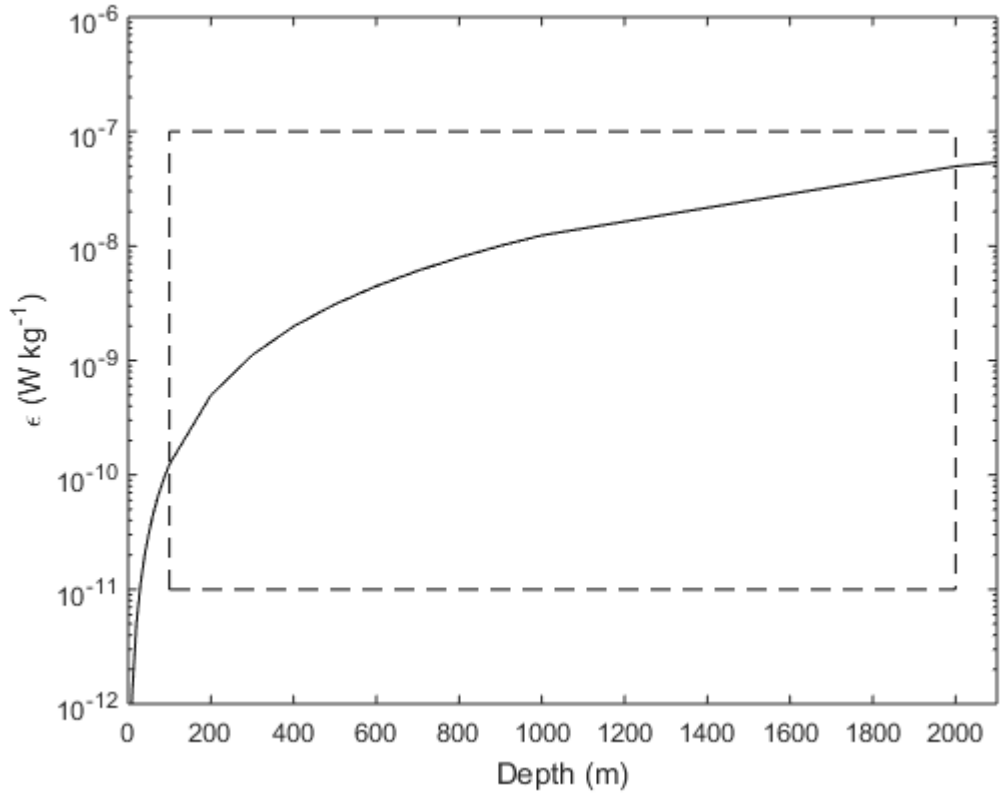

Figure A1: Modeled turbulent energy dissipation rate (ε) using the convective mixing length scale $\tau = 12$ hours [7]. The dashed box represents the approximate range of observed turbulent energy dissipation rates (ε) and vortex depth in deep convection [4,9–11].

Vertical profiles of modelled turbulent diffusivity (K_T)

The vertical profiles of the mean turbulent diffusivity (K_T) within the vortex show lower values at the sea surface, the highest values at around 30% of the depth and the slowest at the bottom (figure A2). These profiles are generally in agreement with those from application of LES used to simulate deep convection [12].

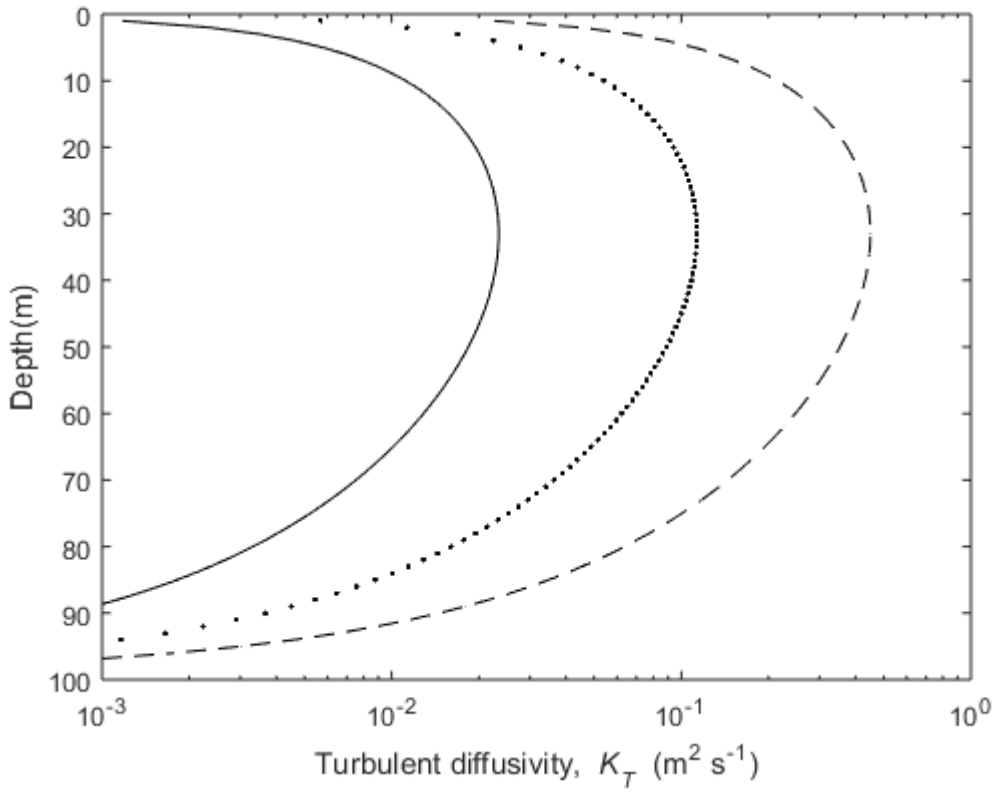

Figure A2: Profiles of turbulent diffusivity (K_T) for a 100 meter deep vortex with mean velocities of 25 m d^{-1} (solid line), 75 m d^{-1} (dotted line) and 200 m d^{-1} (dashed line).

Spatial phytoplankton distribution with horizontally homogenous turbulent diffusivity (K_T)

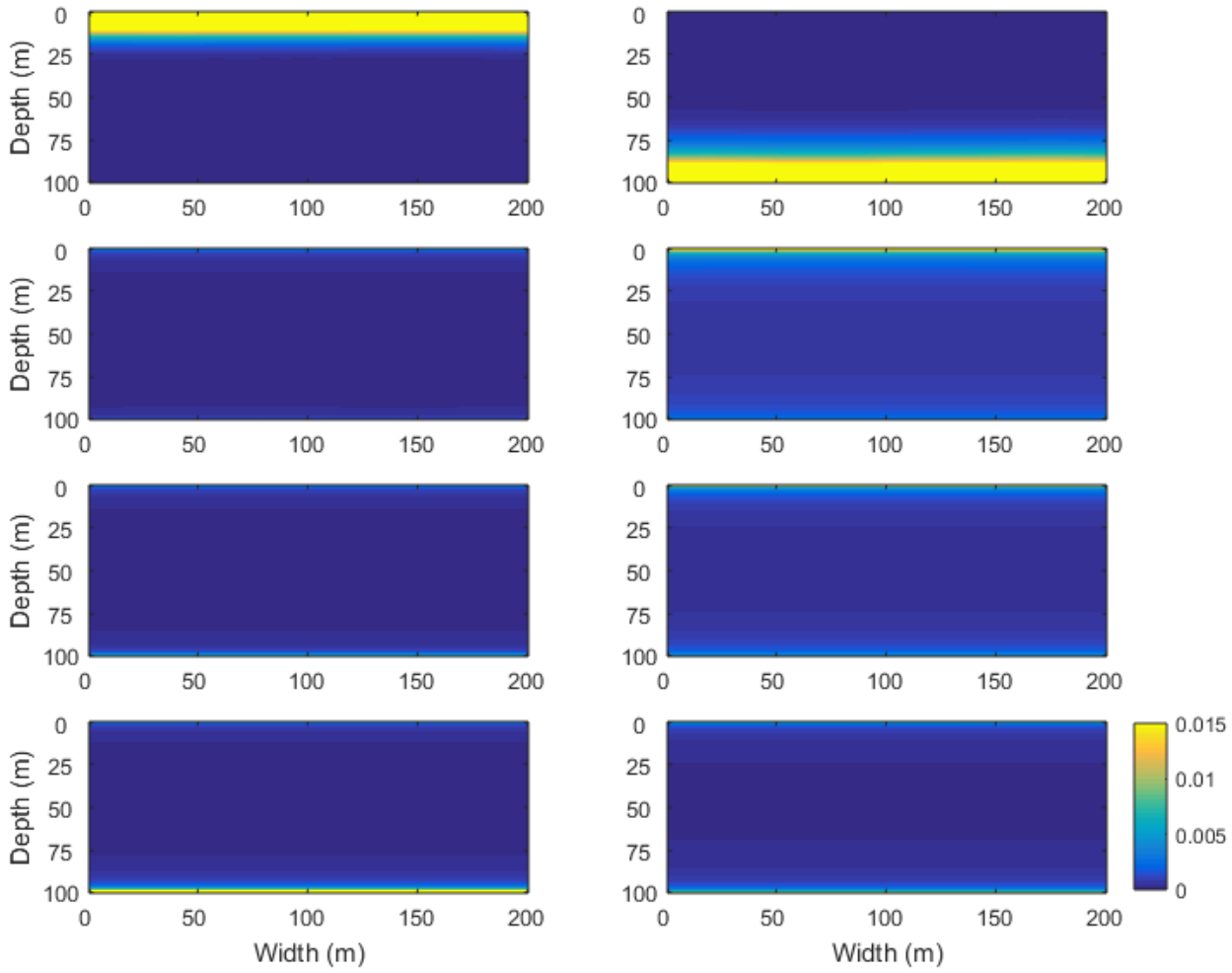

Figure A3: Spatial distribution (right eigenvector of the dominant eigenvalue, v_r) of neutrally buoyant (left column) and fast sinking (10 m d^{-1}, right column) phytoplankton. The maximum flow field velocities are (a,b) 0 m d^{-1}, (c,d) 50 m d^{-1}, (e,f) 200 m d^{-1} and (g,h) 1000 m d^{-1}. The turbulent diffusivity (K_T) is parameterized according to Eq. 7 and the mean vertical profile of K_T is applied homogenously in the horizontal dimension.

Estimates of observed turbulent diffusivity (K_T)

In convective systems K_T can be described using the mean vertical velocity ($\bar{u}$) and the depth of the vortex (h_z) according to Eq. 5 [13].

In figure A4 the black dots show K_T estimated from observed values of $\bar{u}$ and h_z, taken from [13–19]. Lavender et al. [16] found that peak vertical velocities are log normal distributed. Therefore, in convective systems where only the maximum vertical velocity ($u_{\max}$) was available the mean vertical velocity was estimated according to $\bar{u} = 10^{\frac{\log10(u_{\max})}{2}}$.

K_T can also be estimated from the surface buoyancy flux J_0^B, according to [13] $K_T = h_z^{3/4}\left|J_0^B\right|^{1/3}$.

In figure B4 the gray dots show K_T estimated from observed values of J_0^B. In convective system the surface buoyancy flux is related to the net surface heat flux J_0^h (W m^{-2}) through

$J_0^B = \frac{\alpha g}{\rho_0 c_p} J_0^h$, with α (2.5*10^{-4} °C^{-1}) being the thermal expansion coefficient; g (9.81 m^2 s^{-1}) being the gravitational acceleration; ρ_0 (1037 kg m^{-3}) being the seawater density and c_p (3998 J (kg°C)$^{-1}$) being the heat capacity.

Hence, K_T can also be described as a function of J_0^h [20]:

$$K_T = h_z^{3/4}\left|\frac{\alpha g}{\rho_0 c_p} J_0^h\right|^{1/3} \quad \text{(Eq. A4)}$$

In figure A4 the lines indicate theoretical estimates of K_T for different values of J_0^h.

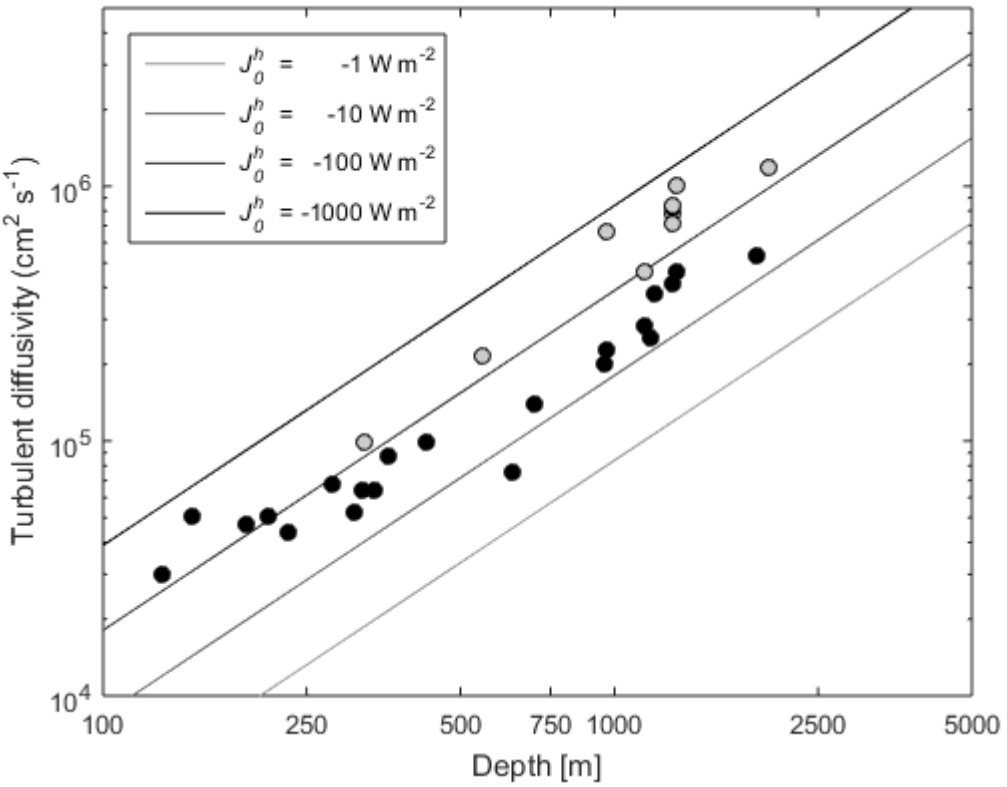

Figure A4: Observed and theoretical estimates of turbulent diffusivity K_T . The black dots are estimated from vertical velocities (Eq. 5), the gray dots are estimated from surface buoyancy flux J_0^B and the lines are theoretical estimates (using Eq. A4) for J_0^h with values -1, -10, -100 and -1000 W m^{-2}.

Net population growth rate and light extinction coefficients

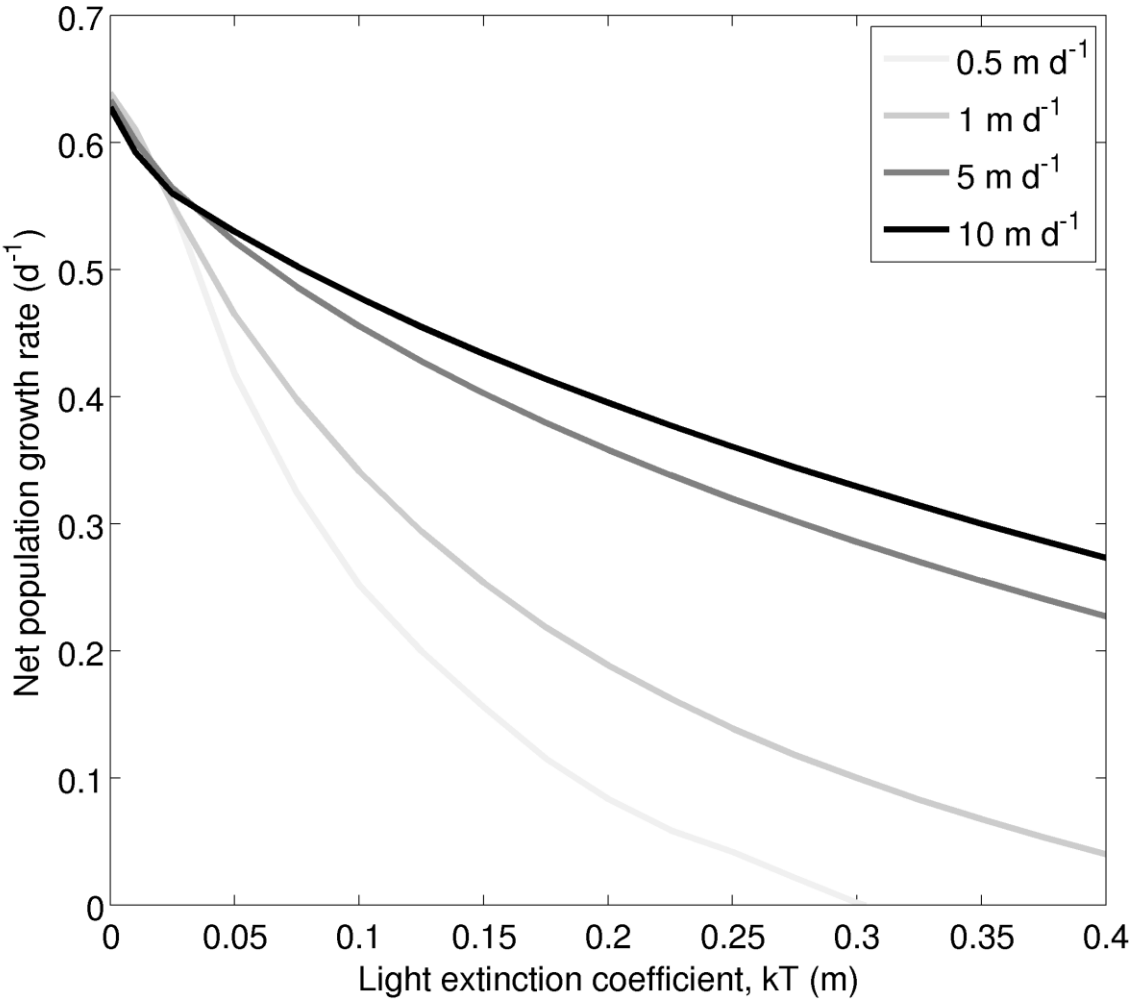

Figure A5: Changes of the net population growth rate with different light extinction coefficients at different levels of turbulent advective transport. The depth of the domain is 100 m. All other parameters are given in table 1.

References

1. Smagorinsky J. 1963 General circulation experiments with premitive equation I. The basic experiment. *Mon. Weather Rev.* **91**, 99–164. (doi:10.1175/1520-0493(1963)091)
2. Smagorinsky J. 2003 Large eddy simulation of complex engineering and geophysical flows. In *Evolution of Physical Oceanography* (eds B Galperin, SA Orszag), pp. 3–36. Cambridge: Cambridge University Press.
3. Csanady GT. 1984 The Free Surface Turbulent Shear layer. *J. Phys. Oceanogr.* **14**, 402–411. (doi:10.1175/1520-0485(1984)014<0402:TFSTSL>2.0.CO;2)
4. Lombardo CP, Gregg MC. 1989 Similarity Scaling of Viscous and Thermal Dissipation in a Convecting Surface Boundary Layer. *J. Geophys. Res.* **94**, 6273–6284. (doi:10.1029/JC094iC05p06273)
5. Driest ER Van. 1956 On Turbulent Flow Near a Wall. *J. Aeronaut. Sci.* **23**, 1007–1011. (doi:10.2514/8.3713)
6. Deardorff JW, Willis GE. 1985 Further results from a laboratory model of the convective planetary boundary layer. *Boundary-Layer Meteorol.* **32**, 205–236. (doi:10.1007/BF00121880)
7. Klinger BA, Marshall J, Send U. 1996 Representation of convective plumes by vertical adjustment. *J. Geophys. Res. Ocean.* **101**, 18175–18182. (doi:10.1029/96JC00861)
8. Vassilicos JC. 2015 Dissipation in Turbulent Flows. *Annu. Rev. Fluid Mech.* **47**, 95–114. (doi:10.1146/annurev-fluid-010814-014637)
9. Shay TJ, Gregg MC. 1984 Turbulence in an Oceanic Convective Mixed Layer. *Nature* **310**, 282–285. (doi:10.1038/310282a0)
10. Shay TJ, Gregg MC. 1986 Convectively Driven Turbulent Mixing in the Upper Ocean. *J. Phys. Oceanogr.* **16**, 1777–1798. (doi:10.1175/1520-0485(1986)016<1777:CDTMIT>2.0.CO;2)
11. Stips A, Burchard H, Bolding K, Eifler W. 2002 Modelling of convective turbulence with a two-equation k-ε turbulence closure scheme. *Ocean Dyn.* **52**, 153–168. (doi:10.1007/s10236-002-0019-2)
12. Taylor JR, Ferrari R. 2011 Shutdown of turbulent convection as a new criterion for the onset of spring phytoplankton blooms. *Limnol. Oceanogr.* **56**, 2293–2307. (doi:10.4319/lo.2011.56.6.2293)

13. Marshall J, Schott F. 1999 Open-ocean convection: Observations, theory, and models. *Rev. Geophys.* **37**, 1–64. (doi:10.1029/98RG02739)
14. Schott F, Visbeck M, Send U, Fischer J, Stramma L, Desaubies Y. 1996 Observations of Deep Convection in the Gulf of Lions, Northern Mediterranean, during the Winter of 1991/92. *J. Phys. Oceanogr.* **26**, 505–524. (doi:10.1175/1520-0485(1996)026<0505:OODCIT>2.0.CO;2)
15. Schott F, Visbeck M, Fischer J. 1993 Observations of Vertical Currents and Convection in the Central Greenland Sea During the Winter of 1988-1989. *J. Geophys. Res.* **98**, 14401–14421. (doi:10.1029/93JC00658)
16. Lavender KL, Davis RE, Owens WB. 2002 Observations of Open-Ocean Deep Convection in the Labrador Sea from Subsurface Floats. *J. Phys. Oceanogr.* **32**, 511–526. (doi:10.1175/1520-0485(2002)032<0511:OOOODC>2.0.CO;2)
17. Steffen EL, D'Asaro EA. 2002 Deep Convection in the Labrador Sea as Observed by Lagrangian Floats. *J. Phys. Oceanogr.* **32**, 475–492. (doi:10.1175/1520-0485(2002)032<0475:DCITLS>2.0.CO;2)
18. D'Asaro EA. 2008 Convection and the seeding of the North Atlantic bloom. *J. Mar. Syst.* **69**, 233–237. (doi:10.1016/j.jmarsys.2005.08.005)
19. Bosse A, Testor P, Mortier L, Prieur L, Taillandier V, D'Ortenzio F, Coppola L. 2015 Spreading of Levantine Intermediate Waters by submesoscale coherent vortices in the northwesternMediterranean Sea as observed with gliders. *J. Geophys. Res. Ocean.* **120**, 1599–1622. (doi:10.1002/2014JC010263)
20. Taylor JR, Ferrari R. 2011 Shutdown of turbulent convection as a new criterion for the onset of spring phytoplankton blooms. *Limnol. Oceanogr.* **56**, 2293–2307. (doi:10.4319/lo.2011.56.6.2293)